Ultrahigh sensitivity of rotation sensing beyond the trade-off between sensitivity and linewidth by the storage of light in a dynamic slow-light resonator

Xuenan Zhang (张学楠),* Yundong Zhang (掌蕴东), He Tian (田赫), Hao Wu (吴昊), Geng Li (李赓), Ruidong Zhu (朱瑞冬), and Ping Yuan (袁萍)

National Key Laboratory of Tunable Laser Technology, Institute of Opto-Electronics, Harbin Institute of Technology, Harbin 150080, People's Republic of China

(Received 30 August 2011; published 9 December 2011)

We propose to employ the storage of light in a dynamically tuned add-drop resonator to realize an optical gyroscope of ultrahigh sensitivity and compact size. Taking the impact of the linewidth of incident light on the sensitivity into account, we investigate the effect of rotation on the propagation of a partially coherent light field in this dynamically tuned slow-light structure. It is demonstrated that the fundamental trade-off between the rotation-detection sensitivity and the linewidth will be overcome and the sensitivity-linewidth product will be enhanced by two orders of magnitude in comparison to that of the corresponding static slow-light structure. Furthermore, the optical gyroscope employing the storage of light in the dynamically tuned add-drop resonator can acquire ultrahigh sensitivity by extremely short fiber length without a high-performance laser source of narrow linewidth and a complex laser frequency stabilization system. Thus the proposal in this paper provides a promising and feasible scheme to realize highly sensitive and compact integrated optical gyroscopes by slow-light structures.

DOI: 10.1103/PhysRevA.84.063823 PACS number(s): 42.81.Pa, 42.60.Da, 42.25.Kb, 42.81.Wg

I. INTRODUCTION

Optical gyroscopes of high sensitivity and compact size have been attracting much investigation interest due to their numerous applications ranging from inertial navigation systems to positioning systems. The Sagnac phase shift accumulated by an electromagnetic wave in a rotation waveguide, which is proportional to the length and the rotation rate of the waveguide [1,2], is the underlying concept for optical gyroscopes to detect rotation velocity. Therefore, to acquire higher sensitivity, one always increases the length of the waveguide of an optical gyroscope. However, to increase the length of the waveguide is less attractive for the practical realization of a highly compact integrated optical gyroscope.

In recent years, many researchers have paid more and more attention to the ultimate control of the group velocity of light, in that slow light has potential applications for the technology of high-capacity optical communication networks [3], image processing [4], optical sensing [5] and measurement [6], optical amplification [7], and quantum information processing [8–10]. A variety of approaches to slow down and even to stop an optical pulse have been developed, since the remarkable ultraslow light at 17 m/s was initially demonstrated by using electromagnetically induced transparency (EIT) in coherent atomic gases [11]. Generally speaking, one can classify these approaches into two categories: atomic resonances and optical resonances. Although the initial ultraslow group velocity and the stopping of optical pulses have been demonstrated in atomic resonances [11–13], the specific wavelength corresponding to the atomic transition, the residual intrinsic absorption of the atomic systems, and the narrow operational bandwidth impose restrictions on further application of the atomic resonances [14]. From the perspective of dispersion engineering, the optical resonances should be an alternative promising approach, because the properties provided can avoid the preceding disadvantages of slow light based on atomic transition [14].

Since slow-light optical resonance structures possess sharp phase shift variation due to high dispersion with compact size, one proposes to utilize dramatic normal dispersion of optical resonance structures to realize highly sensitive and compact optical gyroscopes [15–22]. For example, these optical resonance structures include the side-coupled integrated spaced sequence of resonators (SCISSOR) [16,18], the photonic crystal structure [17], the coupled resonator optical waveguides (CROW) [19], the coupled-resonator-induced transparency (CRIT) structure [20,21], and so on. Moreover, it is experimentally demonstrated that the normal dispersion of the single side-coupled resonator as a basic cell of the preceding optical resonance structures can actually obtain the large differential Sagnac phase shift by short fiber length [23]. Generally, for the optical gyroscope employing the normal dispersion of optical resonance structures (the slow-light resonator structure gyroscopes), the differential Sagnac phase shift is proportional to the photonic coherence-induced group delay or group index of the structures [16,20,23]. Thus, one may design and implement some appropriate optical resonance structures of strong normal dispersion in order to develop a highly sensitive and compact integrated optical gyroscope.

In spite of possessing high sensitivity due to high dispersion, these optical resonance structures, such as slow-light devices, have to suffer the fundamental trade-off between the bandwidth and the group delay [7,24–27] as well as the trade-off between the linewidth of incident light and the differential Sagnac phase shift (proportional to the group delay or the group index [16,20,23]) for rotation sensing. In other words, for the optical gyroscope based on the static optical resonance structures [15–23], the narrow dispersion range due to the large differential Sagnac phase shift or the high sensitivity requires a high-performance laser source of narrow linewidth and a complex laser frequency stabilization system [28], which will increase the enormous

*zhangxuenan@gmail.com

engineering complexity and make the optical gyroscope more unpractical.

In this paper, we first review the fundamental trade-off between the bandwidth and the group delay in some typical optical resonance structures and specifically derive the constraint of the sensitivity-linewidth product (SLP) of the static add-drop resonator configuration in Sec. II. Secondly, in Sec. III, to overcome the drawbacks due to the constraint of the SLP, we propose to employ the storage of light in a dynamically tuned add-drop resonator configuration (a dynamically tuned slow-light structure) to realize an optical gyroscope. Taking the impact of the linewidth of incident light on the sensitivity of the optical gyroscope into account, we investigate the effect of rotation on the propagation of a partially coherent light field in this dynamically tuned slow-light structure. Then, in Sec. IV, we compare the sensitivity of this proposed optical gyroscope with that of the optical gyroscope based on the static single side-coupled resonator [23]. In Sec. IV A, it is demonstrated that the fundamental trade-off between the rotation-detection sensitivity and the linewidth will be overcome. Furthermore, in Sec. IV B, the proposed optical gyroscope can acquire ultrahigh sensitivity by short circumference of fiber length without a high-performance laser source of narrow linewidth and a complex laser frequency stabilization system. Finally, in Sec. V, we compare the ultimate detection sensitivity [28] of the proposed gyroscope employing the storage of light with that of a conventional fiber optic gyroscope (FOG).

II. THE TRADE-OFF RELATION BETWEEN SENSITIVITY AND LINEWIDTH OF STATIC OPTICAL RESONANCE STRUCTURES FOR ROTATION SENSING

Generally, an optical pulse cannot be stopped in a static optical resonance system, since the optical pulse must suffer the fundamental trade-off relation between the bandwidth and the group delay in the static system due to the constraint of the delay-bandwidth product (DBP) [7,24–27]. For example, to avoid the strong distortion of a slow-light pulse in a SCISSOR structure, the delay-bandwidth product (DBP) should satisfy $t_g(\omega_{re})\Delta\nu \leqslant N^{2/3}/6\pi$, where $t_g(\omega_{re})$, $\Delta\nu$, and N represent the group delay at resonant frequency ω_{re}, the bandwidth of incident light pulse, and the number of the resonators in the SCISSOR structure [29]. Similarly, for minimal distortion in a CROW structure, the minimum group velocity of optical pulses is not smaller than $0.01c$ at 10 Gbit/s rate at a wavelength of 1.55 μm [25,27].

Specifically, for a static add-drop resonator configuration [30] (the static single side-coupled ring resonator in Ref. [23] is a specific example of the configuration) as shown in Fig. 1, there also exists a constraint of the delay-bandwidth product. By the coupling matrix formalism [31–33], if the incident light is launched into the port of Add 1, we can deduce the group delay of the static add-drop resonator at the output port of Add 2 as

$$\Delta t_{\mathrm{add}}(\phi) = \frac{\left(1-\rho_1^2\right)a\left[a\left(1+\rho_1^2\right)-\rho_1(1+a^2)\cos(\phi)\right]n_eL}{\left[\rho_1^2+a^2-2\rho_1 a\cos(\phi)\right]\left[\rho_1^2a^2-2\rho_1 a\cos(\phi)+1\right]c}, \quad (1)$$

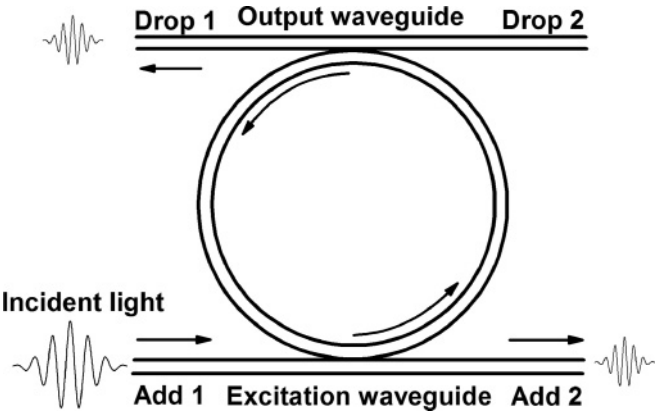

FIG. 1. Schematic of the static add-drop resonator configuration.

where ρ_1, $a = a_0\rho_2$, a_0, ρ_2, $\phi = n_eL/c$, n_e, L, and c denote the transmission coefficient of the excitation waveguide over the coupling length, the general round-trip loss coefficient, the round-trip intrinsic loss coefficient, the transmission coefficient of the output waveguide, the round-trip phase shift, the effective index of the resonator, the circumference of the resonator, and the velocity of light in vacuum, respectively. In the vicinity of the resonant frequency ω_{re}, Eq. (1) can be expanded into the Taylor series as

$$\Delta t_{\mathrm{add}}(\omega) = \Delta t_{\mathrm{add}}(\omega_{re}) + \frac{1}{2!}\frac{d^2\Delta t_{\mathrm{add}}}{d\omega^2}\bigg|_{\omega=\omega_{re}}(\omega-\omega_{re})^2 + \frac{1}{4!}\frac{d^4\Delta t_{\mathrm{add}}}{d\omega^4}\bigg|_{\omega=\omega_{re}}(\omega-\omega_{re})^4+\cdots, \quad (2)$$

where the zero and second derivatives of the group delay on resonance are $\Delta t_{\mathrm{add}}(\omega_{re}) = (n_eL/c)a(1-\rho_1^2)/[(a-\rho_1)(1-a\rho_1)]$ and $(d^2\Delta t_{\mathrm{add}}/d\omega^2)|_{\omega=\omega_{re}} = -(n_eL/c)^3a\rho_1(1-\rho_1^2)[(1-6a^2+a^4)\rho_1+a(1+a^2)(1+\rho_1^2)]/[(a-\rho_1)(1-a\rho_1)]^3$, respectively. If the parameters of the resonator satisfy $a \approx 1$ and $\sqrt{0.5} \leqslant \rho_1 < a$, that is to say, if the resonator is of high quality (Q) factor and normal dispersion, the zero and second order derivatives in Eq. (2) will become $\Delta t_{\mathrm{add}}(\omega_{re}) = (n_eL/c)(1+\rho_1)/(1-\rho_1)$ and $(d^2\Delta t_{\mathrm{add}}/d\omega^2)|_{\omega=\omega_{re}} = -(n_eL/c)^3 2\rho_1(1+\rho_1)/(1-\rho_1)^3$. To prevent the decay of the group delay due to broad bandwidth $\Delta\nu$, the zero- and second-order terms of the group delay should satisfy the condition as $\Delta t_{\mathrm{add}}(\omega_{re}) + 0.5[0.5(2\pi\Delta\nu)](d^2\Delta t_{\mathrm{add}}/d\omega^2)|_{\omega=\omega_{re}} \geqslant 0$, which would lead to the constraint of the DBP as

$$\Delta t_{\mathrm{add}}(\omega_{re})\Delta\nu \leqslant 0.6462. \quad (3)$$

Similarly, if the resonator is of high quality (Q) factor ($a_0 \approx 1$ and $\rho_1, \rho_2 \geqslant \sqrt{0.5}$), one can also deduce the constraint of the DBP at the output port of Drop 1 as

$$\Delta t_{\mathrm{drop}}(\omega_{re})\Delta\nu \leqslant 0.3376. \quad (4)$$

The conditions of $\Delta t_{\mathrm{add}}(\omega_{re})\Delta\nu \leqslant 0.6462$ and $\Delta t_{\mathrm{drop}}(\omega_{re})\Delta\nu \leqslant 0.3376$ indicate the constraint of the DBP in the static add-drop resonator configuration. Therefore, when an optical pulse propagates through the static optical resonance system, it will also suffer the fundamental trade-off between the group delay and the bandwidth.

In addition, if one estimates the strong dispersion range by the full width at half maximum (FWHM) W of the resonance peak of the static add-drop resonator, one can also obtain similar conditions as the trade-off relation between the group delay and the strong dispersion range as $\Delta t_{\mathrm{add}}(\omega_{re})W \leqslant 0.6462$ and $\Delta t_{\mathrm{drop}}(\omega_{re})W \leqslant 0.3376$ in the same situation, where the FWHM is given by $W = (2c/\pi n_e L)\arcsin[(1-a\rho_1)/2\sqrt{a\rho_1}]$.

Once the dramatic normal dispersion of an optical resonance structure is employed to enhance the rotation-dependent phase difference (the differential Sagnac phase shift) and the rotation-detection sensitivity, the fundamental trade-off between the group delay and the bandwidth will transform into the trade-off relation between the sensitivity and the linewidth of incident light in that the enhanced rotation-dependent phase difference and the sensitivity enhancement are generally proportional to the photonic coherence-induced group index or group delay [16,20,23]. Specifically, for an optical gyroscope employing the normal dispersion of a static add-drop resonator, the enhanced rotation-dependent phase difference is $\Delta\Phi'(\omega_0,\Omega) = 2\int_{\Delta\phi^s(\omega_0,0)}^{\Delta\phi^s(\omega_0,\Omega)}[n_g(\Delta\phi^s)/n_e]d\Delta\phi^s$. Additionally, the rotation-detection sensitivity enhancement factor η' [22,23], which is the ratio between the rotation-dependent phase difference of the gyroscope and that of a conventional fiber optic gyroscope with equal fiber length and equal footprint, is [23]

$$\eta'_{\mathrm{add(drop)}}(\omega_0,\Omega) = \int_{\Delta\phi^s(\omega_0,0)}^{\Delta\phi^s(\omega_0,\Omega)}[n_g(\Delta\phi^s)/n_e]d\Delta\phi^s \Big/ \int_{\Delta\phi^s(\omega_0,0)}^{\Delta\phi^s(\omega_0,\Omega)} d\Delta\phi^s, \tag{5}$$

where ω_0, Ω, $n_g = c\Delta t_{\mathrm{add(drop)}}/L$, $\Delta t_{\mathrm{add(drop)}}$, and $\Delta\phi^s$ are the angular frequency of monochromatic incident light, the clockwise rotation angular velocity of the static add-drop resonator, the group index, the group delay, and the Sagnac phase shift accumulated by the clockwise light wave in the conventional FOG with equal fiber length and equal footprint, respectively. Apparently η' approximates n_g/n_e at a slow rotation rate $\Omega(\to 0)$.

According to Eqs. (3)–(5), the constraint of the sensitivity-linewidth product (SLP) at the output port of Add 2 and Drop 1 can be derived as

$$\eta'_{\mathrm{add}}(\omega_{re},0)\Delta \leqslant 0.6462, \tag{6}$$

and

$$\eta'_{\mathrm{drop}}(\omega_{re},0)\Delta \leqslant 0.3376, \tag{7}$$

where $\Delta = \Delta\nu_{in}/\Delta\nu_{\mathrm{FSR}}$ as the ratio of the linewidth $\Delta\nu_{in}$ of incident light to the free spectral range $\Delta\nu_{\mathrm{FSR}} = c/n_e L$ is the dimensionless parameter of linewidth. The conditions of Eqs. (6) and (7) indicate that the gyroscope employing the normal dispersion of the static add-drop resonator will suffer the trade-off relation between the sensitivity and the linewidth. As a result, if a laser source with broad linewidth is launched into this static slow-light resonator structure gyroscope, the high sensitivity (the large sensitivity enhancement factor η') may not be obtained due to the trade-off relation despite the strong normal dispersion. Thus, when one wants to obtain high rotation-detection sensitivity by this gyroscope, the narrowness of the structure bandwidth due to the high sensitivity (the large sensitivity enhancement factor η') will require a high-performance laser source of narrow linewidth and a complex laser frequency stabilization system [28]. In brief, the trade-off relation between the sensitivity and the linewidth not only may limit further sensitivity enhancement of the static slow-light resonator structure gyroscope but also increases the engineering complexity and makes the gyroscope system unpractical.

To overcome the preceding shortcomings due to the trade-off relation between the sensitivity and the linewidth, one may use a dynamic optical resonance structure to obtain a large SLP for rotation sensing. The dynamic optical resonance structure with a large SLP can balance between the sensitivity and the linewidth and hence may acquire higher rotation-detection sensitivity by shorter fiber length without a high-performance laser source of narrow linewidth and a complex laser frequency stabilization system, which is attractive for the realization of a highly compact and sensitive optical gyroscope. On the other hand, to evaluate the effectiveness of a slow-light resonator structure gyroscope, only the sensitivity (the sensitivity enhancement factor) is not enough and the SLP is another significant parameter.

III. ROTATION SENSING BEYOND THE TRADE-OFF RELATION BETWEEN SENSITIVITY AND LINEWIDTH BY STORAGE OF LIGHT

To obtain ultrahigh sensitivity (the sensitivity enhancement factor) of a slow-light resonator structure gyroscope beyond the preceding trade-off relation between the sensitivity and the linewidth, we propose to employ the storage of light in the dynamically tuned add-drop resonator (a dynamically tuned slow-light structure) in Fig. 2 to obtain a large SLP. For concreteness, while the structure is rotated, one needs to compress the bandwidth of the structure reversibly [7,24–27] or dynamically tune the quality (Q) factor [34,35] of the ring resonator of the structure as the three following sequential steps: Step 1. Couple light through Coupler 1 into the resonator (the resonator is an open cavity with broad bandwidth and low Q factor Q_1). Step 2: Store light in the resonator (the resonator is a closed cavity with narrow bandwidth and higher Q factor Q_2). Step 3: Release the stored light through Coupler

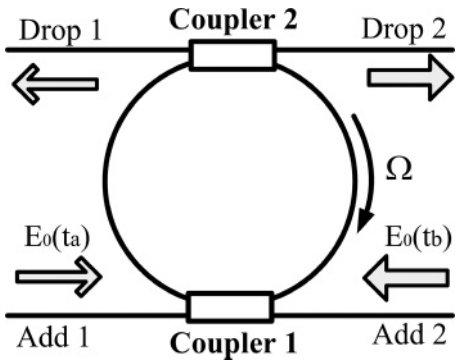

FIG. 2. Schematic of the dynamically tuned add-drop resonator configuration used for rotation sensing.

2 with high coupling efficiency (the resonator turns back to be an open cavity with broader bandwidth and lower Q factor Q_3, $Q_2 > Q_1 > Q_3$). To perform the preceding operation, we propose to modulate the coupling coefficients of Coupler 1 and Coupler 2 in time. Suppose $\kappa_1(t)$ and $\kappa_2(t)$ are the time-varying coupling coefficients of Coupler 1 and Coupler 2 and t_i is the duration time of Step i. In Step 1 corresponding to the time interval $[-t_1,0]$, we assume that the coupling coefficients are $|\kappa_1^2(t)| = 0.05$ and $|\kappa_2^2(t)| = 0$. Hence the counterpropagating incident light waves from the ports of Add 1 and Add 2 as shown in Fig. 2 are coupled into the ring resonator through Coupler 1. Afterwards, at the beginning of Step 2 (at time $t = 0$), the stepwise modulation of Coupler 1 is switched on with $|\kappa_1^2(t)| = 0$. In Step 2 of the time interval $[0,t_2]$, one should retain $|\kappa_1^2(t)| = 0$ and $|\kappa_2^2(t)| = 0$ so as to close the ring resonator. Thus the intracavity light waves captured in Step 1 are trapped and stored in the rotated and closed resonator. Finally, at the beginning of Step 3 (at time $t = t_2$), the stepwise modulation of Coupler 2 is switched off with $|\kappa_2^2(t)| = 0.5$. In Step 3 of the time interval $[t_2,t_2 + t_3]$, since $|\kappa_1^2(t)| = 0$ and $|\kappa_2^2(t)| = 0.5$, the stored counter-rotating light waves are released through Coupler 2 into the ports of Drop 1 and Drop 2 to sense rotation by their rotation-dependent phase difference. In brief, $\kappa_1(t)$ and $\kappa_2(t)$ are vanishing except $|\kappa_1^2(t)| = 0.05$ for $-t_1 \leqslant t \leqslant 0$ and $|\kappa_2^2(t)| = 0.5$ for $t_2 \leqslant t \leqslant t_3$, and the process of the modulations on $\kappa_1(t)$ and $\kappa_2(t)$ in the three steps are illustrated by Fig. 3(a).

To accomplish the preceding tuning steps, one may fabricate the ring resonator of the dynamically tuned add-drop resonator structure by single-mode optical fiber and two (2×2) optical fiber couplers (Coupler 1 and Coupler 2) with time-varying coupling coefficients. In practice, one can utilize the ultrafast (2×2) silicon electric-optic switch based on a Mach-Zehnder interferometer (MZI) [36,37] to realize the coupler with a time-varying coupling coefficient. In Refs. [36,37], when the phase of the MZI is tuned by the free carrier-induced index change due to forward-biased drive voltage modulation on the p-i-n junction in the MZI, the functionality of the (2×2) coupler with a time-varying coupling coefficient can be realized.

To quantify the process further and take the effect of linewidth of incident light on the rotation-detection sensitivity into account, let us assume that the polychromatic incident light is a partially coherent Gaussian wave [38,39] with the duration $T_0(<t_1)$ and the central angular frequency ω_0 corresponding to the wavelength of 1550 nm as

$$\begin{aligned}\Gamma_0(t_a,t_b) &= \langle E_0(t_a)E_0(t_b)\rangle_e \\ &= A_0 \exp\left(-\frac{t_a^2 + t_b^2}{2T_0^2}\right) \exp\left[-\frac{(t_a - t_b)^2}{2T_c^2}\right] \\ &\quad \times \exp[i(\omega_0 t_a - \omega_0 t_b)], \end{aligned} \tag{8}$$

where T_c is the coherence temporal length and $\langle\cdots\rangle_e$ denotes the ensemble average over different realizations of the pulse [38,39]. The linewidth that can be evaluated by the FWHM spectral width of the incident light is $\Delta\nu_{in} = [(T_c^2 + 2T_0^2)ln2]^{0.5}/T_0T_c\pi$ if $T_0 \gg T_c$.

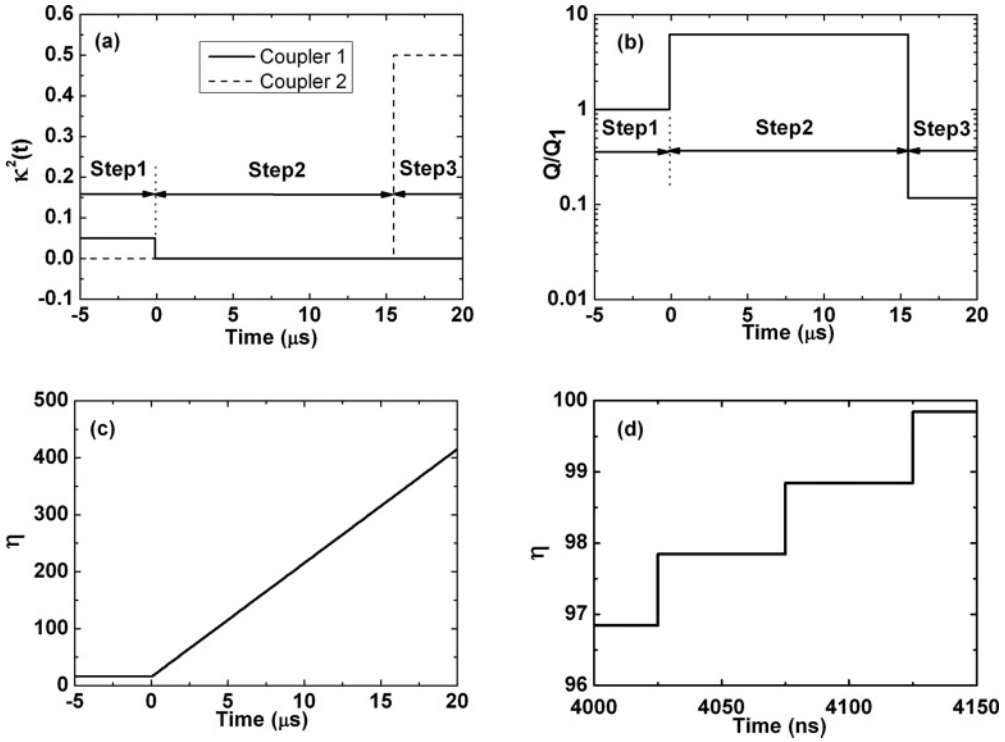

FIG. 3. (a) Temporal evolution of the coupling strengths $\kappa_1^2(t)$ (solid curve) and $\kappa_2^2(t)$ (dashed curve). (b) Temporal evolution of the relative quality factor Q/Q_1 of the dynamically tuned add-drop resonator. (c) Temporal evolution of the rotation-detection sensitivity enhancement factor $\eta(t)$ of the dynamically tuned add-drop resonator. (d) Expanded view of $\eta(t)$ for 4 μs $\leqslant t \leqslant$ 4.15 μs. The parameters are $T_0 = 35.355$ μs, $\Delta\nu_{in} = 5.30$ MHz, $L = 10$ m, $N = 10$, $n_e = 1.5$, $a_0 = 0.9952$, $\Omega = 0.0157$ rad/s, and $t_2 = 15.546$ μs $\approx 3\tau_2$.

In Step 1, when the polychromatic incident light waves represented by Eq. (8) from the ports of Add 1 and Add 2 are being coupled into and captured by the rotating ring resonator in Fig. 2, the rotation will modify the phases along the loops of the resonator accumulated by counter-rotating light waves and hence will induce the corresponding phase difference accumulated along the loops. Furthermore, as a result of the photonic coherence-induced steep normal dispersion in the vicinity of resonant frequency ω_{re}, the rotation-dependent phase difference between the counter-rotating intracavity light waves will be enhanced with respect to the phase difference accumulated along the loops [20–23]. To calculate the enhanced rotation-dependent phase difference accumulated in Step 1, the cross correlation $\Gamma(t,t) = \langle [E^-(t)]^* E^+(t)\rangle_e$ $(-t_1 \leqslant t \leqslant 0)$ describing the evolution of the counter-rotating intracavity light fields $E^+(t)$ and $E^-(t)$ at Coupler 1 can be used and given by the following inverse Fourier transformation:

$$\Gamma(t,t) = \int\int_0^\infty d\omega d\omega' W(\omega,\omega') \exp[i(\omega t - \omega' t)] \times T_1[\phi(\omega') + \Delta\phi^s(\omega',\Omega)] T_1^*[\phi(\omega) - \Delta\phi^s(\omega,\Omega)], \tag{9}$$

where T_1 and $W(\omega,\omega')$ are the dispersion relation and the cross-spectral density of the incident light, respectively. The dispersion relation is $T_1(\phi) = \kappa_1(t)/[1 - a\rho_1(t)\exp(i\phi)]$, where $\rho_1(t) = [1-\kappa_1^2(t)]^{0.5}$, $a = a_0\rho_2(t)$, a_0, and $\rho_2(t) = [1-\kappa_2^2(t)]^{0.5}$ are the transmission coefficient of Coupler 1, the general round-trip loss coefficient, the round-trip intrinsic loss coefficient, and the transmission coefficient of Coupler 2, respectively. And the cross-spectral density that can be deduced from the Fourier transformation of Eq. (8) is $W(\omega_a,\omega_b) = (A_0 T_0/2\pi\Delta\omega)\exp[-(\omega_a-\omega_0)^2/2\Delta\omega^2 - (\omega_b-\omega_0)^2/2\Delta\omega^2]$ $\exp[-(\omega_b-\omega_a)^2/2\Delta\omega_c^2]$, where $\Delta\omega = \sqrt{1/T_0^2 + 2/T_c^2}$ and $\Delta\omega_c = (T_c/T_0)\Delta\omega$ characterize the spectral linewidth and the degree of spectral coherence [39]. In Eq. (9), $[\phi(\omega) \pm \Delta\phi^s(\omega,\Omega)]$ as the round-trip phases accumulated along the loops consist of both the propagation phase $\phi(\omega) = \omega n_e L/c$ and the rotation-modified (Sagnac) phase shifts $\pm\Delta\phi^s(\omega,\Omega) = \pm 2\omega\pi R^2\Omega N/c^2$ for clockwise (+) and counterclockwise (–) light waves due to the Sagnac effect, where n_e, L, c, Ω, N, and $R = L/2\pi N$ represent the dispersion-free effective index of the resonator, the total circumference of the ring resonator, the velocity of light in vacuum, the clockwise angular velocity of the resonator, the loop number of the resonator, and the radius of the loop, respectively. According to Eq. (9), the enhanced rotation-dependent phase difference (differential Sagnac phase shift) between the counter-rotating intracavity light waves accumulated in Step 1 can be represented by the angle of the correlation $\Delta\Phi(t) = \arg[\Gamma(t,t)]$ $(-t_1 \leqslant t \leqslant 0)$ and the rotation-detection sensitivity enhancement factor [22,23] (in comparison to a conventional FOG with equal fiber length and same footprint) is related as $\eta(t) = \Delta\Phi(t)/2\Delta\phi^s(\omega_0,\Omega)$ $(-t_1 \leqslant t \leqslant 0)$ for the general case of polychromatic incident light. For monochromatic incident light in Step 1, $\eta(t)$ reduces to Eq. (5), only if the group index is substituted by $n_{g1}(\phi) = (c/L)[\partial \arg(T_1)/\partial\omega] = n_e a\rho_1(t)[\cos\phi - a\rho_1(t)]/[1 - 2a\rho_1(t)\cos\phi + a^2\rho_1^2(t)]$ in Eq. (5). If the incident light is slowly time-varying, $\Delta\Phi(t)$ and $\eta(t)$ in Step 1 are approximately time independent in that the resonator is still a static resonator in Step 1. For example, in Fig. 3(c), $\eta(t)$ is approximately a constant $(16.29 \leqslant \eta(t) \leqslant 16.40)$ for $-5\ \mu s \leqslant t \leqslant 0$ in Step 1.

Subsequently, in Step 2, when the counter-rotating intracavity light waves captured by the ring resonator in Step 1 are stored and propagate in the rotating and closed resonator, the Sagnac phase shift continues to be accumulated in addition to the enhanced phase shift obtained in Step 1 and the intracavity light intensity will decay slowly without coupling loss. (Here the active optical fiber can be used to fabricate the resonator to reduce the loss and increase the photon lifetime further [40,41]). In Step 3, when the stored light waves in Step 2 are released through Coupler 2, the counter-rotating intracavity light waves that determine the property of the released light waves will also acquire the additional Sagnac phase shifts due to the nonvanishing photon lifetime in this release step. Accordingly, in Steps 2 and 3 for $0 < t \leqslant t_2 + t_3$, the cross correlation of the counter-rotating intracavity light waves at Coupler 2 becomes

$$\Gamma(t,t) = \Gamma(t - \Delta t^-, t - \Delta t^+)\exp\{-[\theta(t) + \theta(t_2 - t)]t/2\tau_2\} \times \exp[-\theta(t-t_2)(t-t_2)/\tau_3], \tag{10}$$

where $\tau_2 = Q_2/\omega_0 = -n_e L/2c\ln a_0$ and $\tau_3 = Q_3/\omega_0 = n_e L/c\kappa_2^2(t) - n_e L/2c\ln a_0$ are the intracavity photon lifetimes of Steps 2 and 3, $\theta(t)$ is the stepwise function and $\Delta t^\pm$ denotes the rotation-modified delay times of the clockwise (+) and counterclockwise (–) intracavity light waves. The first term on the right-hand side of Eq. (10), which can be calculated by Eq. (9), indicates that the intracavity light waves in Steps 2 and 3 evolve from the intracavity light waves captured by the ring resonator in Step 1. The rotation-modified delay times $\Delta t^\pm = n_e L(M + 0.5)/c \pm LR\Omega(M + 0.5)/c^2$ (M satisfies $n_e L(M - 0.5)/c < t \leqslant n_e L(M + 0.5)/c$ and is a positive integer), that approximate $\Delta t^\pm \approx n_e L(M + 0.5)/c \pm tR\Omega/n_e c$ once $t \gg n_e L/c$, can be obtained by integrating the rotation-modified delay time differential equation [20]:

$$dt = (Rd\theta/c)[\beta' + n_e(\omega) + (\beta - \beta')\omega n_e(\omega)(\partial n_e/\partial\omega) + (\beta - \beta')n_e(\omega)^2], \tag{11}$$

where we assume that $\beta = \Omega R/c$ and $\beta' = \Omega_m R/c$ as the relative velocities of the resonator and the filling medium are equal and the medium is free of dispersion $(\partial n_e/\partial\omega = 0)$. According to Eq. (10), the rotation-dependent phase difference between the counter-rotating intracavity light waves and the rotation-detection sensitivity enhancement factor are still related as $\Delta\Phi(t) = \arg[\Gamma(t,t)]$ and $\eta(t) = \Delta\Phi(t)/2\Delta\phi^s(\omega_0,\Omega)$ in the case of polychromatic incident light in Steps 2 and 3 for $0 < t \leqslant t_2 + t_3$, respectively.

Indeed, for $n_e L/c \ll t \leqslant t_2 + t_3$, the rotation-dependent phase difference $\Delta\varphi(\omega,t) = \omega(\Delta t^+ - \Delta t^-) \approx 2\omega t R\Omega/n_e c$ at a specific frequency ω accumulated in Steps 2 and 3 is approximately proportional to the time t in the long time range. It is an intuitive result, since the propagation distance on which the Sagnac effect depends in Steps 2 and 3 is determined by the time t during which the intracavity light waves are trapped in the resonator. Moreover, the impact

of the linewidth $\Delta\nu_{in}$ of incident light on the rotation-dependent phase difference $[\Delta\Phi(t) - \Delta\Phi(0)]$ accumulated in Steps 2 and 3 is negligible, since the relative deviation of $\Delta\varphi(\omega,t)$ caused by the linewidth $\Delta\nu_{in}$ can satisfy $[\Delta\nu_{in}/\Delta\varphi(\omega_0,t)]d\Delta\varphi(2\pi\nu,t)/d\nu = 2\pi\Delta\nu_{in}/\omega_0 \ll 1$ generally and the narrow-band cavity buildup $|T_1^2|$ in Step 1 may reduce the impact further. Therefore, the rotation-dependent phase difference $[\Delta\Phi(t) - \Delta\Phi(0)]$ of polychromatic light accumulated in Steps 2 and 3 will be determined only by the trapped time t in the long time range and may not be influenced by linewidth and the constraint of the SLP.

As shown in Fig. 3(c), the numerical simulation of Eq. (10) demonstrates that the rotation-detection sensitivity enhancement factor $[\eta(t) - \eta(0)]$ (proportional to the rotation-dependent phase difference $[\Delta\Phi(t) - \Delta\Phi(0)]$) of polychromatic light accumulated in Steps 2 and 3 will actually increase linearly approximately in time despite $\Delta\nu_{in} \gg W$, where W represents the FWHM spectral width of the add-drop resonator in Step 1 ($W = 0.19$ MHz for the parameters in Fig. 3). Also, the result in Fig. 3(c) indicates that the optical gyroscope employing the storage of light in the dynamically tuned add-drop resonator may acquire ultrahigh sensitivity as ultrahigh $\eta(t_2 + t_3)$ beyond the trade-off relation between the sensitivity and the linewidth, since only $\eta(t_2) = 326.90$ in Fig. 3(c) is much larger than the maximum rotation-detection sensitivity enhancement factor $\max(\eta') = 80.86$ of the corresponding static single side-coupled resonator with equal fiber length and same footprint in the case of monochromatic incident light.

IV. COMPARISON BETWEEN A DYNAMICALLY TUNED ADD-DROP RESONATOR AND A STATIC SINGLE SIDE-COUPLED RESONATOR FOR ROTATION SENSING

According to the preceding analysis, the total rotation-detection sensitivity enhancement factor of the optical gyroscope based on the dynamically tuned add-drop resonator obtained after the three tuning steps is $\eta(t_2 + t_3)$, which is determined by the photonic-induced dispersion relation T_1, the storage time t_2, and the release time t_3. Thus the optical gyroscope may acquire ultrahigh sensitivity beyond the constraint of the SLP only if the moderate dispersion T_1 is implemented and the moderate t_2 and t_3 are chosen. To demonstrate this viewpoint, we will closely compare the rotation-detection sensitivity enhancement factor, the SLP, and the detuning property of the optical gyroscope employing the storage of light in the dynamically tuned add-drop resonator with those of the optical gyroscope based on the static single side-coupled resonator [23] with equal total circumference and same resonator footprint, since the static single side-coupled resonator is a specific example of the static add-drop resonator.

For the static single side-coupled resonator, the property of the dispersion is determined by the coupling regime. In the over-coupled regime ($\rho' < a_0'$) [42,43], the photonic coherence-induced normal dispersion that can be used to enhance the sensitivity of optical gyroscopes occurs. When the counterpropagating polychromatic incident light waves represented by Eq. (8) are launched into the rotated resonator from Ports 1 and 2 as shown in Fig. 4, the rotation will result in the differential Sagnac phase shift between counter-rotating

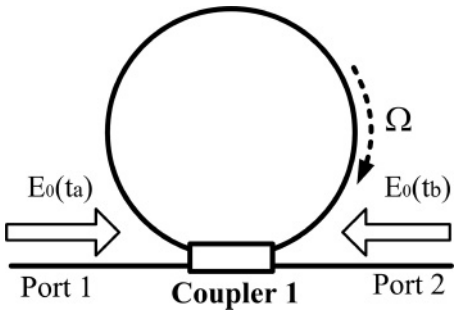

FIG. 4. Schematic of the static single side-coupled resonator used for rotation sensing.

light waves accumulated in the loops of the resonator and the photonic coherence-induced normal dispersion will enhance the phase difference. The enhanced rotation-dependent phase difference (differential Sagnac phase shift) $\Delta\Phi'$ can also be calculated by the angle of the cross correlation represented by Eq. (9) only if the dispersion relation is substituted by $T'(\phi) = [\rho' - a_0' \exp(i\phi)]/[1 - a_0'\rho' \exp(i\phi)]$, where a_0' and ρ' are the round-trip intrinsic loss coefficient and the transmission coefficient of Coupler 1. Moreover, the parameters with the superscript such as $\Delta\Phi'$, a_0', ρ', and T' are the corresponding parameters of the static single side-coupled resonator; for instance, $\kappa' = \sqrt{1 - (\rho')^2}$, n_e', L', Ω', W', ω_{re}', N', $R' = L'/2\pi N'$, and η' represent the coupling coefficient of Coupler 1, the effective index, the total circumference, the clockwise rotation angular velocity, the FWHM spectral width, the resonant frequency, the loop number, the radius of the loop, and the rotation-detection sensitivity enhancement factor of the static single side-coupled resonator, respectively.

A. Comparison of dependence of sensitivity on linewidth

Figure 5(a) illustrates the dependence of the rotation-detection sensitivity enhancement factor on the linewidth of incident light for the gyroscope employing the storage of light in the dynamically tuned add-drop resonator and the gyroscope based on the static single side-coupled resonator with equal total circumference ($L = L' = 10$ m) and same footprint ($N = N' = 10, R = R'$). To prevent too much loss of light intensity in Steps 2 and 3, we choose the storage time $t_2 = 15.546\ \mu s \approx 3\tau_2$ and the release time $t_3 = 0.051\ \mu s \approx 0.5\tau_3$ for the parameters of the dynamically tuned add-drop resonator in Fig. 5. When the linewidth of incident light $\Delta\nu_{in}$ satisfies $0 \leqslant \Delta\nu_{in} \leqslant W = W' = 0.19$ MHz, the rotation-detection sensitivity enhancement factor $\eta(t_2 + t_3)$ of the gyroscope based on the dynamically tuned add-drop resonator that will satisfy $336.85 \leqslant \eta(t_2 + t_3) \leqslant 343.81$ is boosted by at least three times with respect to the rotation-detection sensitivity enhancement factor η' ($46.76 \leqslant \eta' \leqslant 80.86$) of the gyroscope based on the static single side-coupled resonator. If the linewidth increases further in Fig. 5(a), the sensitivity enhancement factor of the dynamically tuned add-drop resonator will decrease slightly whereas that of the static single side-coupled resonator will drop rapidly. When 0.19 MHz $< \Delta\nu_{in} <$ 20 MHz, despite the slight decay of $\eta(t_2 + t_3)$ the dynamically tuned add-drop resonator is more superior to the static single side-coupled resonator,

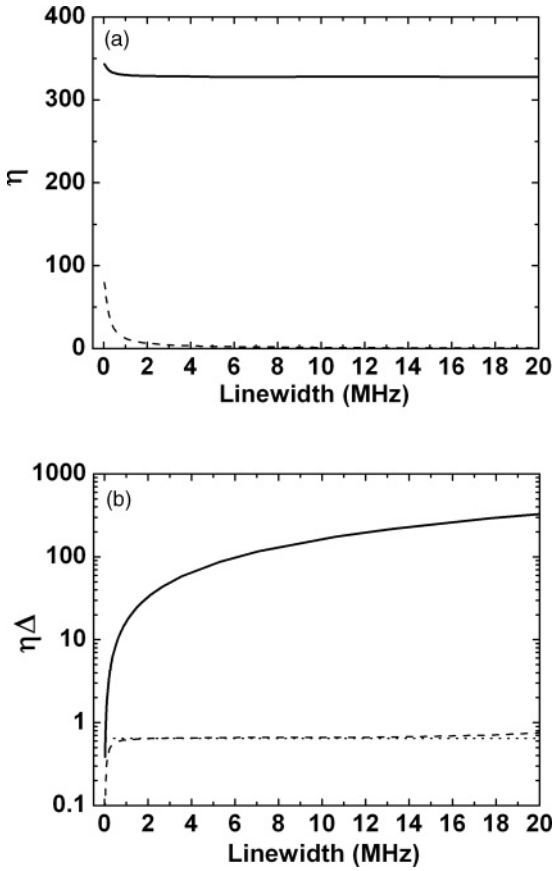

FIG. 5. (a) The rotation-detection sensitivity enhancement factor $\eta(\eta')$ versus the linewidth $\Delta\nu_{in}$ of incident light. (b) The SLP $\eta\Delta(\eta'\Delta)$ versus the linewidth $\Delta\nu_{in}$. The solid and dashed curves represent the dynamically tuned add-drop resonator and the static single side-coupled resonator, respectively. The parameters of the dynamically tuned add-drop resonator are $L = 10$ m, $N = 10$, $n_e = 1.5$, $a_0 = 0.9952$, $\Omega = 0.0157$ rad/s, $t_2 = 15.546\ \mu$s, $t_3 = 0.051\ \mu$s, and $\omega_0 = \omega_{re}$. The parameters of the static single side-coupled resonator are $L' = 10$ m, $N' = 10$, $n'_e = 1.5$, $a'_0 = 0.9952$, $\Omega' = 0.0157$ rad/s, $\omega_0 = \omega'_{re}$, and $|\kappa'|^2 = 0.05$, which are similar to those of the dynamically tuned add-drop resonator. The dotted curve in Fig. 5(b) denotes the constraint value (0.6462) of the SLP of the static single side-coupled resonator represented by Eq. (6).

since $\eta(t_2 + t_3)$ of the dynamically tuned add-drop resonator that satisfies $327.87 \leqslant \eta(t_2 + t_3) \leqslant 336.85$ is at least seven times larger than η' $(0.7524 \leqslant \eta' \leqslant 46.76)$ of the static single side-coupled resonator. Therefore, in contrast to the gyroscope based on the static single-coupled resonator, the gyroscope based on the dynamically tuned add-drop resonator is more sensitive, especially in the case of broad linewidth.

Moreover, as shown in Fig. 5(b), when the linewidth increases and satisfies $\Delta\nu_{in} \leqslant 0.39$ MHz, the SLP $\eta'\Delta$ of the static single side-coupled resonator will arise and be smaller than the constraint value 0.6462 of SLP due to small linewidth. When the linewidth increases further and satisfies $0.39\ \text{MHz} \leqslant \Delta\nu_{in} \leqslant 20$ MHz, the SLP $\eta'\Delta$ $(0.5520 \leqslant \eta'\Delta \leqslant 0.7529)$ of the static single side-coupled resonator will be in the vicinity of the constraint value 0.6462 of the SLP and hence the trade-off relation between the sensitivity and the linewidth will occur. However, for the gyroscope based on the dynamically tuned add-drop resonator, when the linewidth increases and satisfies $\Delta\nu_{in} \leqslant 0.39$ MHz, the SLP $\eta(t_2 + t_3)\Delta$ will rise and be larger than that of the static single side-coupled resonator. When the linewidth increases further and satisfies $0.39\ \text{MHz} \leqslant \Delta\nu_{in} \leqslant 20$ MHz, the SLP $\eta(t_2 + t_3)\Delta$ $[6.50 \leqslant \eta(t_2 + t_3)\Delta \leqslant 328.11]$ is boosted by at least one order of magnitude with respect to the constraint value 0.6462 of the SLP. This result indicates that the trade-off relation between the sensitivity and the linewidth is overcome due to the large SLP of the dynamically tuned add-drop resonator. Thus, the optical gyroscope employing the storage of light in the dynamically tuned add-drop resonator can acquire higher sensitivity without a high-performance laser source of narrow linewidth $\Delta\nu_{in}(\leqslant W)$, which is necessary for the optical gyroscope based on the static single side-coupled resonator [23], other slow-light structures [15–22,28], and a resonant fiber optic gyroscope (RFOG) [28].

B. Comparison of dependence of sensitivity on frequency detuning

It is interesting to note that the gyroscope employing the storage of light in the dynamically tuned add-drop resonator can also acquire ultrahigh and uniform sensitivity irrespective of arbitrary frequency detuning. When the linewidth $\Delta\nu_{in}$ approaches the free spectral range $\Delta\nu_{\text{FSR}}$ of the dynamically tuned add-drop resonator $(\Delta\nu_{in} \sim \Delta\nu_{\text{FSR}})$, the incident light field will be resonant with at least one resonance mode of the ring resonator for arbitrary frequency detuning. Moreover, Fig. 5 shows that the optical gyroscope based on the dynamically tuned add-drop resonator can actually acquire ultrahigh sensitivity and a large SLP on resonance $(\omega_0 = \omega_{re})$ in the case of $\Delta\nu_{in} \sim \Delta\nu_{\text{FSR}}$. Thus it is possible to obtain ultrahigh and uniform sensitivity at arbitrary frequency detuning for the optical gyroscope in the case of $\Delta\nu_{in} \sim \Delta\nu_{\text{FSR}}$.

As illustrated by Fig. 6(a), the numerical simulation of Eq. (10) indicates that, if the linewidth of incident light approaching the free spectral range $\Delta\nu_{\text{FSR}} = 19.99$ MHz is $\Delta\nu_{in} = 17.67$ MHz, the optical gyroscope employing the storage of light in the dynamically tuned add-drop resonator possessing the SLP of 289.86 as shown in Fig. 5(b) will actually acquire the ultrahigh and uniform sensitivity. When the detuning $(\omega_0 - \omega_{re})/2\pi$ varies from -25 MHz to $+25$ MHz (this variation range exceeds $\Delta\nu_{\text{FSR}} = 19.99$ MHz), the rotation-detection sensitivity enhancement factor $\eta(t_2 + t_3)$ that satisfies $327.30 \leqslant \eta(t_2 + t_3) \leqslant 327.43$ will be at least four times as large as the maximum sensitivity enhancement factor $\max(\eta') = 80.86$ of the static single side-coupled resonator with equal total circumference $(L = L' = 10$ m) and same footprint $(N = N' = 10, R = R')$ as shown in Fig. 6(a), and the fluctuation of $\eta(t_2 + t_3)$ will be $<0.1\%$ of its maximum $(\max[\eta(t_2 + t_3)] = 327.43)$ at resonance $(\omega_0 = \omega_{re})$. However, for the optical gyroscope based on the static single side-coupled resonator with similar parameters, one can only obtain high sensitivity as $31.48 \leqslant \eta' \leqslant 80.86$ provided that the detuning is less than the half of the FWHD spectral width of the resonator as $(1/2)W' = 0.09695$ MHz in Fig. 6(a).

In other words, when the dynamically tuned add-drop resonator and the static single side-coupled resonator with equal total circumference $(L = L' = 10$ m) and same footprint

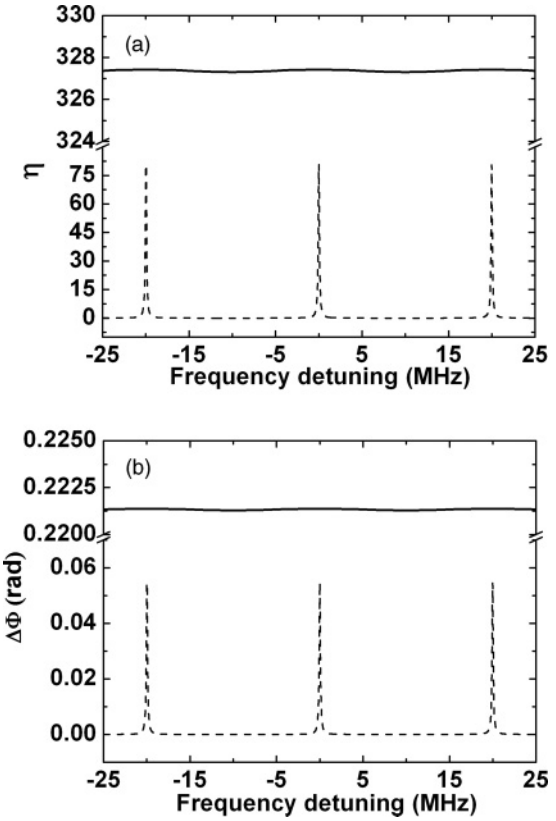

FIG. 6. (a) Dependence of the rotation-detection sensitivity enhancement factor $\eta(\eta')$ on the frequency detuning. (b) Dependence of the rotation-dependent phase difference $\Delta\Phi(\Delta\Phi')$ on the frequency detuning. The solid and dashed curves represent the dynamically tuned add-drop resonator and the static single side-coupled resonator, respectively. The parameters of the dynamically tuned add-drop resonator are $L = 10$ m, $N = 10$, $n_e = 1.5$, $a_0 = 0.9952$, $\Omega = 0.0157$ rad/s, $t_2 = 15.546\ \mu$s, $t_3 = 0.051\ \mu$s, and $\Delta\nu_{in} = 17.67$ MHz. The parameters of the static single side-coupled resonator are $L' = 10$ m, $N' = 10$, $n'_e = 1.5$, $a'_0 = 0.9952$, $\Omega' = 0.0157$ rad/s, and $|\kappa'|^2 = 0.05$, and the incident light wave is a monochromatic light wave.

$(N = N' = 10, R = R')$ in Fig. 6 are rotated at $\Omega = 0.0157$ rad/s, the dynamically tuned add-drop resonator can obtain the rotation-dependent phase difference $2\Delta\phi^s(\omega_0,\Omega) \times \min[\eta(t_2+t_3)] = \min[\Delta\Phi(t_2+t_3)] = 0.2213$ at least and can maintain the ultrahigh phase difference as $0.2213 \leqslant \Delta\Phi(t_2 + t_3) \leqslant 0.2214$ at arbitrary detuning as shown by the solid curve of Fig. 6(b), where $2\Delta\phi^s(\omega_0,\Omega) = 0.0006761$ is the phase difference of the conventional FOG with equal total circumference and the same footprint. However, for the static single side-coupled resonator, the maximum rotation-dependent phase difference is only $\max(\Delta\Phi') = 0.05467$. Moreover, once the detuning of a monochromatic incident light wave exceeds half of the FWHD $(1/2)W' = 0.09695$ MHz, one can only obtain the small phase difference as $\Delta\Phi' \leqslant 0.02128$ that is less than half of its maximum $\max(\Delta\Phi') = 0.05467$ as shown by the dashed curve of Fig. 6(b). Thus it indicates that the optical gyroscope based on the dynamically tuned add-drop resonator can acquire and maintain ultrahigh and uniform sensitivity for an arbitrary detuning and hence does not require a complex laser frequency stabilization system which is necessary for the optical gyroscopes based on the static single side-coupled resonator [23], other slow-light structures [15–22,28], and an RFOG [28].

In practice, the gyroscope based on the dynamically tuned add-drop resonator is feasible even though the response time of the modulation on the coupling coefficient $\kappa_i(t)$ $(i = 1,2)$ is nonvanishing or the modulation is not perfectly stepwise. Assume that t_1^{re} and t_2^{re} are the response times of the modulations on $\kappa_1(t)$ and $\kappa_2(t)$, respectively. In time domain, the nonvanishing t_1^{re} and t_2^{re} result in the time-dependent intensity and phase changes of the counter-rotating intracavity light waves in the response time t_i^{re} $(i = 1,2)$ with respect to those in the case of the stepwise modulation considered here. However, since the ultrafast (2×2) silicon electric-optic switch [36,37] provides such a short response time (< 4 ns [36] and ~ 6 ns [37]) that even satisfies $t_i^{re} \ll n_e L/c \ll \tau_i$ $(i = 1,2)$ ($n_e L/c$, τ_1, and τ_2 are the round-trip time of the resonator, the intracavity photon lifetime in Step 1, and the intracavity photon lifetime in Step 2; in Figs. 3, 5, and 6, $n_e L/c \approx 50$ ns, $\tau_1 = n_e L/c\kappa_1^2(t) - n_e L/2c \ln a = 0.8385\ \mu$s, and $\tau_2 = 5.174\ \mu$s), the time-dependent intensity and phase shift changes will occur in such a short time range (t_i^{re}) that a large proportion $[(n_e L/c) - t_i^{re}]$ of the intracavity light field will not be influenced. In frequency domain, the time-dependent intensity and phase changes can induce the additional spectrum broadening $\Delta\nu$ in Steps 2 and 3, which may result in the deviation of $\Delta\varphi(\omega,t)$ and then retard sensitivity enhancement. Since the relative deviation of $\Delta\varphi(\omega,t)$ caused by $\Delta\nu(\sim 1/t_i^{re})$ due to t_i^{re} (several nanoseconds [36,37]) is approximately $[\Delta\nu/\Delta\varphi(\omega_0,t)]d\Delta\varphi(2\pi\nu,t)/d\nu \approx 2\pi\Delta\nu/\omega_0 \sim 10^{-5}$ at the wavelength of 1550 nm, the impact of the spectrum broadening on the sensitivity can be negligible. Thus the stepwise tuning on the coupling strength considered in the present paper is feasible in practice.

In addition, the further improvement of the SLP and the differential Sagnac phase shift of the optical gyroscope employing the storage of light in the dynamically tuned add-drop resonator can be foreseeable. For instance, one can fabricate the ring resonator of the dynamically tuned add-drop resonator by the active optical fiber [40,41] or by introducing the intracavity dispersion [34,44–46] in order to obtain longer intracavity photon lifetime. Due to the longer lifetime, one may increase the storage time t_2 moderately to acquire higher sensitivity η and a larger SLP. On the other hand, if the optical gyroscope possesses a constant SLP C in some specific situations approximately, we can deduce the formulas as

$$\Delta\Phi(t)\Delta\nu_{in} \leqslant C(c/Ln_e)4\omega\pi R^2\Omega N/c^2, \tag{12}$$

or

$$\Delta\Phi(t) \leqslant CF4\omega\pi R^2\Omega N/c^2, \tag{13}$$

where $F = \Delta\nu_{\mathrm{FSR}}/W$ is the finesse of the resonator. According to the conditions of Eqs. (12) and (13), increasing the circumference of the dynamically tuned ring resonator moderately can also enhance the differential Sagnac phase shift of the optical gyroscope with a constant SLP. Thus, a more sensitive optical gyroscope employing the storage of light can be expected by optimizing the photon lifetime and the

circumference of the dynamically tuned resonator. On the other hand, longer intracavity photon lifetime and larger circumference of the resonator will actually reduce the impact of the nonvanishing response times t_1^{re} and t_2^{re} on the gyroscope further.

It is important to note the implication of the rotation-detection sensitivity enhancement factor η [22,23]. In the present paper, we always refer to the rotation-detection sensitivity enhancement factor η of a slow-light resonator structure gyroscope as the sensitivity or rotation-detection sensitivity for simplicity. The rotation-detection sensitivity enhancement factor η, which is the ratio between the differential Sagnac phase shift of a slow-light resonator structure gyroscope and that of a conventional FOG with equal fiber length and the same footprint, describes the enhancement of the differential Sagnac phase shift under the condition of equal fiber length and the same footprint. Thus it is not only related to sensitivity of a slow-light resonator structure gyroscope under the constraint of equal fiber length and the same footprint but is generally also inversely proportional to the requirement of fiber length for this slow-light resonator structure gyroscope. That is to say, the benefit of a large η of a slow-light resonator structure gyroscope lies in the realization of a highly sensitive and compact integrated optical gyroscope with short fiber length. Therefore the gyroscope based on the dynamically tuned add-drop resonator has the potential of further miniaturization in contrast to the gyroscope based on the static single side-coupled resonator, since the dynamically tuned add-drop resonator can acquire the higher rotation-detection sensitivity enhancement factor η than the static single side-coupled resonator with equal fiber length and the same footprint as shown in Fig. 6.

V. THE ULTIMATE DETECTION SENSITIVITY OF THE GYROSCOPE BASED ON A DYNAMICALLY TUNED ADD-DROP RESONATOR IN COMPARISON TO A CONVENTIONAL FOG

Besides the rotation-detection sensitivity enhancement factor describing the potential of miniaturization, there is another distinct concept of sensitivity as the ultimate detection sensitivity which can be utilized to investigate the superiority of the ultimate theoretical sensitivity of a slow-light resonator structure gyroscope in contrast with a conventional FOG [28]. The ultimate detection sensitivity of a slow-light resonator structure gyroscope is determined by and proportional to the differential Sagnac phase shift of the gyroscope under the constraint of given propagation loss of light field and given resonator footprint [28]. Apparently the constraint of the ultimate detection sensitivity is different from that of the rotation-detection sensitivity enhancement factor we used in the present paper. Moreover, it has been proven that the static CROW gyroscope (a static slow-light resonator structure gyroscope) which can reduce the requirement of fiber length due to the large rotation-detection sensitivity enhancement factor $(1/2\kappa)$ does not enhance the ultimate detection sensitivity beyond that of a conventional FOG [28]. Even though the parameters of the static CROW gyroscope are optimized, the optimized CROW gyroscope consisting of one ring that resembles a RFOG has only the approximately same ultimate detection sensitivity as an "equivalent" conventional FOG, since the differential Sagnac phase shifts of them are approximately equal under the constraint of equal propagation loss of light field and the same footprint [28].

Thus, to evaluate the enhancement of the ultimate detection sensitivity of the gyroscope employing the storage of light in the proposed dynamically tuned add-drop resonator in the present paper with respect to a conventional FOG, one can also compare the differential Sagnac phase shift of the gyroscope with that of a conventional FOG with equal propagation loss and the same footprint.

One first needs to calculate the differential Sagnac phase shift accumulated by the gyroscope based on the dynamically tuned add-drop resonator. In Step 1, the differential Sagnac phase shift can be derived by the equation $\Delta\Phi(t,\omega_0,\Omega) = 2\int_{\Delta\phi^s(\omega_0,0)}^{\Delta\phi^s(\omega_0,\Omega)} [n_g(\Delta\phi^s)/n_e]d\Delta\phi^s \quad (t<0)$ in the case of monochromatic incident light, where the group index in Step 1 is $n_{g1}(\phi) = n_e a_0\rho_{11}[\cos\phi - a_0\rho_{11}]/[1-2a_0\rho_{11}\cos\phi + a_0^2\rho_{11}^2]$ and ρ_{11} denotes the transmission coefficient of Coupler 1 in Step 1. If the incident light field is resonant with one resonance mode of the ring resonator and the resonator is of high quality factor (the round-trip intrinsic loss coefficient a_0 approaches 1), the differential Sagnac phase shift accumulated in Step 1 will approximate $\Delta\Phi(t,\omega_0,\Omega) = \frac{4\pi R^2 N\omega_0\Omega\rho_{11}}{c^2(1-\rho_{11})} \quad (t<0)$. Moreover, in Steps 2 and 3, as is shown in Sec. III, the additional differential Sagnac phase shift determined by the storage time t_2 and the release time t_3 is approximately $2R\Omega\omega_0(t_2+t_3)/n_e c$. Therefore, one can obtain the total differential Sagnac phase shift as $\Delta\Phi(t_2+t_3,\omega_0,\Omega) = \frac{4\pi R^2 N\omega_0\Omega\rho_{11}}{c^2(1-\rho_{11})} + \frac{2R\Omega\omega_0(t_2+t_3)}{n_e c}$ after the three steps.

To guarantee the equal propagation loss on the condition of equal incident power and a given loss coefficient, the loop number N_{FOG} and the loop radius R_{FOG} of the "equivalent" conventional FOG will satisfy $N_{\mathrm{FOG}}R_{\mathrm{FOG}} = \frac{NR\rho_{11}}{(1-\rho_{11})} + \frac{c(t_2+t_3)}{2\pi n_e}$, since it takes $\frac{\rho_{11}}{(1-\rho_{11})}$ and $\frac{c(t_2+t_3)}{2\pi RNn_e}$ times for the resonant incident light field to go around the dynamically tuned add-drop resonator in Step 1 and in Steps 2 and 3, respectively. Moreover, the requirement for the same footprint yields the condition as $\pi R_{\mathrm{FOG}}^2 = \pi R^2$. Under the preceding two conditions, one may compare the differential Sagnac phase shift $[\Delta\Phi(t_2+t_3,\omega_0,\Omega)]$ of the gyroscope based on the dynamically tuned add-drop resonator with that $(\Delta\Phi_{\mathrm{FOG}}(\omega_0,\Omega) = 4\pi R_{\mathrm{FOG}}^2 N_{\mathrm{FOG}}\omega_0\Omega/c^2)$ of the "equivalent" conventional FOG to evaluate the enhancement of the ultimate detection sensitivity of the former.

After the comparison, it is shown that the differential Sagnac phase shifts of them are indeed equal. Thus, the proposed gyroscope based on the dynamically tuned add-drop resonator has about the same ultimate detection sensitivity as a conventional FOG and an RFOG under the constraint of equal propagation loss of light field and the same footprint. Nevertheless, in contrast to a conventional FOG and an RFOG, the proposed gyroscope based on the dynamically tuned add-drop resonator can acquire the approximately same ultimate detection sensitivity by shorter fiber length due to its higher rotation-detection sensitivity enhancement factor η.

In the present paper, we do not aim to explore a slow-light resonator structure gyroscope with enhanced ultimate detection sensitivity but to explore a slow-light structure gyroscope

with a larger sensitivity-linewidth product (SLP) in order to overcome the fundamental trade-off between the rotation-detection sensitivity enhancement factor (η) and the linewidth. When the SLP of the proposed gyroscope using the storage of light in the dynamically tuned add-drop resonator is enormously enhanced in comparison to the SLP of the gyroscope based on the corresponding static resonator, the proposed gyroscope not only can acquire ultrahigh differential Sagnac phase shift by shorter fiber length due to higher η and hence has the potential of further miniaturization, but also does not require a high-performance laser source of narrow linewidth, a complex laser frequency stabilization system, or even a stringent control of optical path of the resonator. Whereas, for a static slow-light resonator structure gyroscope and an RFOG, a high-performance laser source of narrow linewidth, a complex laser frequency stabilization system, and a stringent control of optical path of the resonator which significantly increase engineering complexity are necessary and at the expense of miniaturization of a static slow-light resonator structure gyroscope and an RFOG [28]. Thus, the gyroscope employing the storage of light in the dynamically tuned add-drop resonator with a large SLP, which can acquire ultrahigh sensitivity by the gyroscope system of further miniaturization and can overcome the disadvantages of a static slow-light structure gyroscope and an RFOG due to their miniaturization, enables the highly sensitive optical gyroscopes of compact size by slow-light structures to become more promising and feasible in practice.

VI. CONCLUSION

We propose to dynamically compress the bandwidth of the add-drop resonator reversibly or dynamically tune the quality (Q) factor of this slow-light structure to realize the storage of light for rotation sensing. This proposal provides a scheme to realize an optical gyroscope of ultrahigh sensitivity and compact size beyond the fundamental trade-off relation of the sensitivity and the linewidth. In contrast to the static single side-coupled resonator with equal total circumference and footprint, when the incident linewidth approaches the free spectral range, the optical gyroscope based on this proposed scheme can acquire higher and more uniform rotation-detection sensitivity without a high-performance laser source of narrow linewidth, a complex laser frequency stabilization system, or even a stringent control of optical path of the resonator, since the SLP of the optical gyroscope based on this proposed scheme is enhanced by at least two orders of magnitude with respect to the constraint of the SLP of the optical gyroscope based on the static single side-coupled resonator. It implies that the single side-coupled resonator [23] of higher Q factor [34] and even other optical resonance structures [15–22] (slow-light resonator structures) with stronger photonic coherence-induced dispersion and narrower dispersion range may be improved and utilized as a miniature gyroscope for high-precision rotation sensing by the scheme. Therefore, the proposed scheme enables the highly sensitive and compact integrated optical gyroscopes by slow-light structures [15–23] to become more promising and feasible in practice.

ACKNOWLEGMENT

This research is supported by the National Natural Science Foundation of China (NSFC) under Grants No. 61078006 and No. 60878006.

[1] E. J. Post, Rev. Mod. Phys. **39**, 475 (1967).
[2] H. J. Arditty and H. C. Lefovre, Opt. Lett. **6**, 401 (1981).
[3] R. Ramaswami and K. N. Sivarajan, *Optical Networks: A Practical Perspective* (Morgan Kaufmann, San Francisco, 1998).
[4] R. M. Camacho, C. J. Broadbent, I. Ali-Khan, and J. C. Howell, Phys. Rev. Lett. **98**, 043902 (2007).
[5] M. Terrel, M. J. F. Digonnet, and S. H. Fan, Appl. Opt. **48**, 4874 (2009).
[6] Z. Shi, R. W. Boyd, R. M. Camacho, P. K. Vudyasetu, and J. C. Howell, Phys. Rev. Lett. **99**, 240801 (2007).
[7] S. Sandhu, M. L. Povinelli, and S. H. Fan, Appl. Phys. Lett. **95**, 081103 (2009).
[8] M. D. Lukin and A. Imamoglu, Nature (London) **413**, 273 (2001).
[9] L. M. Duan, M. D. Lukin, J. I. Cirac, and P. Zoller, Nature (London) **414**, 413 (2001).
[10] M. Fleischhauer and M. D. Lukin, Phys. Rev. A **65**, 022314 (2002).
[11] L. V. Hau, S. E. Harris, Z. Dutton, and C. H. Behroozi, Nature (London) **397**, 594 (1999).
[12] C. Liu, Z. Dutton, C. H. Behroozi, and L. V. Hau, Nature (London) **409**, 490 (2001).
[13] D. F. Phillips, A. Fleischhauer, A. Mair, R. L. Walsworth, and M. D. Lukin, Phys. Rev. Lett. **86**, 783 (2001).
[14] L. Maleki, A. B. Matsko, A. A. Savchenkov, and V. S. Ilchenko, Opt. Lett. **29**, 626 (2004).
[15] M. S. Shahriar, G. S. Pati, R. Tripathi, V. Gopal, M. Messall, and K. Salit, Phys. Rev. A **75**, 053807 (2007).
[16] A. B. Matsko, A. A. Savchenkov, V. S. Ilchenko, and L. Maleki, Opt. Commun. **233**, 107 (2004).
[17] B. Z. Steinberg, Phys. Rev. E **71**, 056621 (2005).
[18] A. B. Matsko, A. A. Savehenkov, V. S. Ilchenko, and L. Maleki, Opt. Commun. **259**, 393 (2006).
[19] J. Scheuer and A. Yariv, Phys. Rev. Lett. **96**, 053901 (2006).
[20] C. Peng, Z. B. Li, and A. S. Xu, Appl. Opt. **46**, 4125 (2007).
[21] C. Peng, Z. B. Li, and A. S. Xu, Opt. Express **15**, 3864 (2007).
[22] J. Scheuer, Opt. Lett. **34**, 1630 (2009).
[23] Y. D. Zhang, H. Tian, X. N. Zhang, N. Wang, J. Zhang, H. Wu, and P. Yuan, Opt. Lett. **35**, 691 (2010).
[24] Q. Xu, P. Dong, and M. Lipson, Nat. Phys. **3**, 406 (2007).
[25] M. F. Yanik and S. H. Fan, Phys. Rev. Lett. **92**, 083901 (2004).
[26] M. F. Yanik, W. Suh, Z. Wang, and S. H. Fan, Phys. Rev. Lett. **93**, 233903 (2004).
[27] M. F. Yanik and S. H. Fan, Phys. Rev. A **71**, 013803 (2005).

[28] M. A. Terrel, M. J. F. Digonnet, and S. H. Fan, J. Lightwave Technol. **27**, 47 (2009).
[29] J. B. Khurgin and P. A. Morton, Opt. Lett. **34**, 2655 (2009).
[30] B. E. Little, S. T. Chu, H. A. Haus, J. Foresi, and J. P. Laine, J. Lightwave Technol. **15**, 998 (1997).
[31] L. F. Stokes, M. Chodorow, and H. J. Shaw, Opt. Lett. **7**, 288 (1982).
[32] J. E. Heebner and R. W. Boyd, Opt. Lett. **24**, 847 (1999).
[33] J. K. S. Poon, J. Scheuer, S. Mookherjea, G. T. Paloczi,Y. Huang, and A. Yariv, Opt. Express **12**, 90 (2004).
[34] Y. Dumeige, S. Trebaol, and P. Feron, Phys. Rev. A **79**, 013832 (2009).
[35] H. N. Yum, M. E. Kim, Y. J. Jang, and M. S. Shahriar, Opt. Express **19**, 6705 (2011).
[36] J. V. Campenhout, W. M. J. Green, S. Assefa, and Y. A. Vlasov, Opt. Express **17**, 24020 (2009).
[37] P. Dong, S. R. Liao, H. Liang, R. Shafiiha, D. Z. Feng, G. L. Li, X. Z. Zheng, A. V. Krishnamoorthy, and M. Asghari, Opt. Express **18**, 25225 (2010).
[38] P. Paakkonen, J. Turunen, P. Vahimaa, A. T. Friberg, and F. Wyrowski, Opt. Commun. **204**, 53 (2002).
[39] H. Lajunen, J. Turunen, P. Vahimaa, J. Tervo, and F. Wyrowski, Opt Commun. **255**, 12 (2005).
[40] J. M. Choi, R. K. Lee, and A. Yariv, Opt. Lett. **26**, 1236 (2001).
[41] Y. Dumeige, T. K. N. Nguyen, L. Ghisa, S. Trebaol, and P. Feron, Phys. Rev. A **78**, 013801 (2008).
[42] J. E. Heebner, V. Wong, A. Schweinsberg, R. W. Boyd, and D. J. Jackson, IEEE J. Quantum Electron. **40**, 726 (2004).
[43] D. D. Smith and H. R. Chang, J. Mod. Opt. **51**, 2503 (2004).
[44] G. Müller, M. Müller, A. Wicht, R.-H. Rinkleff, and K. Danzmann, Phys. Rev. A **56**, 2385 (1997).
[45] M. D. Lukin, M. Fleischhauer, M. O. Scully, and V. L. Velichansky, Opt. Lett. **23**, 295 (1998).
[46] M. Soljačić, E. Lidorikis, L. V. Hau, and J. D. Joannopoulos, Phys. Rev. E **71**, 026602 (2005).